Journal for Multiscale Computational Engineering, 11 (1): 17–26 (2013)

BUCKLING PROPERTIES OF PRE-STRESSED MULTI-WALLED CARBON NANOTUBES

Ming D. Ma,[1,] Luming Shen,[2] Lifeng Wang,[3] & Quanshui Zheng[1]*

[1]*Department of Engineering Mechanics, Tsinghua University, Beijing 100084, China*

[2]*School of Civil Engineering, University of Sydney, NSW 2006, Australia*

[3]*Department of Mechanical Engineering, Massachusetts Institute of Technology, Cambridge, Massachusetts 02139, USA*

[*]Address all correspondence to Ming D. Ma, E-mail: morning22704@gmail.com

Pre-stressed multi-walled carbon nanotubes (PS-MWCNTs) have (a) interwall distances less than 0.34 nm, (b) highest Young's moduli, and (c) interlayer shear strengths several orders higher than those of normal MWCNTs. In this paper, the buckling behaviors of PS-MWCNTs with two to six layers have been studied using both molecular mechanics simulation and continuum mechanics models. Considering the interlayer distance as the key factor, we reveal three features of the buckling behavior of PS-MWCNTs subjected to axial loading: (1) the buckling membrane force is not a monotonic function of interlayer distance, depending on the nanotube index (i.e. diameter); (2) the buckling membrane force increases as the interlayer distance decreases for PS-MWCNTs with fixed intertube chirality, which is a combined effect of interlayer distance and tube diameter; and (3) for PS-MWCNTs with the same innermost tube, the buckling membrane force increases as the number of walls increases. Furthermore, molecular mechanics simulation and the multi-shell continuum model agree on the trend of the buckling membrane force as a function of interlayer distance, tube chirality index, and number of layers. These results can serve as a bridge between the molecular simulation and the continuum model for the buckling behaviors of PS-MWCNT.

KEY WORDS: *pre-stressed carbon nanotube, interlayer distance, buckling, molecular mechanics simulation, continuum model*

1. INTRODUCTION

Carbon nanotubes (CNTs) have held the promise of materials with the highest Young's modulus (∼1 TPa) (Mielke et al., 2007) owing to the strong sp^2 bond since the their discovery in 1976 (Oberlin et al., 1976). The inter-layer shear strength, however, is extremely small (0.08–0.3 MPa) (Cumings and Zettl, 2000; Yu et al., 2000a, 2000b) which results in poor inter-layer load transfer, and becomes the primary obstacle on fabricating CNT-reinforced composites with proposed excellent mechanical performance (Xu et al., 2008).

In order to improve the inter-layer load-transfer properties of multi-walled carbon nanotubes, two methods have been proposed. One is to introduce crosslinks between neighboring layers, named the crosslink mechanism (da Silva et al., 2005; Kis et al., 2004; Xia et al., 2007), which could increase the bending modulus by up to 30 fold (Kis et al., 2004). However, the drawback of the crosslink methods is that the accompanying defects, which are inherent for this method, in the CNTs so produced have greatly reduced tensile strength, thus severely harming their mechanical properties (Kis et al., 2004; Mielke et al., 2004; Sammalkorpi et al., 2004). In contrast to the crosslink method, the second method—decreasing the distance between layers, resulting in the so-called pre-stressed multi-walled carbon nanotube (PS-MWCNT)—could increase the inter-layer load-transfer ability by up to four orders while maintaining the Young's modulus as well as leaving the strength unchanged (Xu et al., 2008). Besides that, the fabrication of PS-MWCNTs has been partially accomplished (Ma et al., 2010; Sun et al., 2006).

1543–1649/13/$35.00

Although several mechanical properties of PS-MWCNTs have been well studied (Ma et al., 2010; Xu et al., 2008), the bucking properties of PS-MWCNTs have been investigated to a very limited degree (Liew et al., 2007; Wang et al., 2010; Wang, 2006; Zhang et al., 2007). Wang et al. found that the critical buckling stress and buckling strain of double-walled PS-MWCNTs are greatly enhanced using molecular mechanics (MM) simulation (Wang, 2006). Using the structure parameters derived from MM simulation as the input data for continuum mechanics (CM) model, Liew et al. (2007) have obtained similar enhancements in buckling behaviors of PS-MWCNTs as compared to normal MWNTs. Similar results are found by Zhang et al. (2007) in the study of buckling behavior of four PS-DWCNTs using MM simulation. In this paper, we first study PS-DWCNTs with the same inner tube but different interlayer distances, and find that the buckling force increases with decreasing interlayer distance, as concluded by other researchers (Liew et al., 2007; Wang, 2006; Zhang et al., 2007). Next, by extending our simulation model to PS-DWCNTs with different inner tubes and PS-MWCNTs with 3 to 6 layers, we find that the monotonic relation does not hold any more. Also we find that the buckling membrane force increases as the interlayer distance decreases for PS-MWCNTs with a fixed intertube chirality difference. For PS-MWCNTs with the same innermost tube, the buckling membrane force increases as the number of walls increases. Finally, we compare our simulation results directly with continuum model (He et al., 2005a; 2005b) using the same procedure as described by (Liew et al., 2007). In addition to validating the three buckling properties proposed based on our MM simulation, to our surprise, we find that the buckling force predicted by CM model is almost proportional to that calculated by MM simulation. In the end, we point out the significance of the agreement between MM simulation and CM model.

2. MOLECULAR MECHANICS (MM) SIMULATION MODEL

In our MM simulations, the second-generation reactive empirical bond order (REBO) potential (Brenner et al., 2002) and its extension (Stuart et al., 2000), which can predict the mechanical properties of CNTs correctly (Huhtala et al., 2004), is adopted to model carbon–carbon interaction. The LAMMPS package (Plimpton, 1995) is used throughout our simulation.

The MM simulation configuration is shown in Fig. 1(a). Before applying any load, we conduct energy minimization using the conjugate gradient method to determine the initial balanced configuration of PS-MWCNTs. After that, we fix one end of the tubes, and compress the other end by 0.001 nm in each time step. We then fix both ends of the tubes and relax all other carbon atoms of the tubes to their new equilibrium positions by minimizing the potential energy of the system. By repeating such displacement-controlled loading, we are able to simulate the buckling behavior of PS-MWCNTs and obtain the buckling configuration and the corresponding buckling force, F_{MM}, as demonstrated in Figs. 1(b) and 1(c), respectively. The corresponding buckling membrane force, N_{MM}, is then calculated by $N_{MD} = F_{MD}/\sum_{i=1}^{N} 2\pi R_i$, where R_i is the radius of the ith layer counting from the inner.

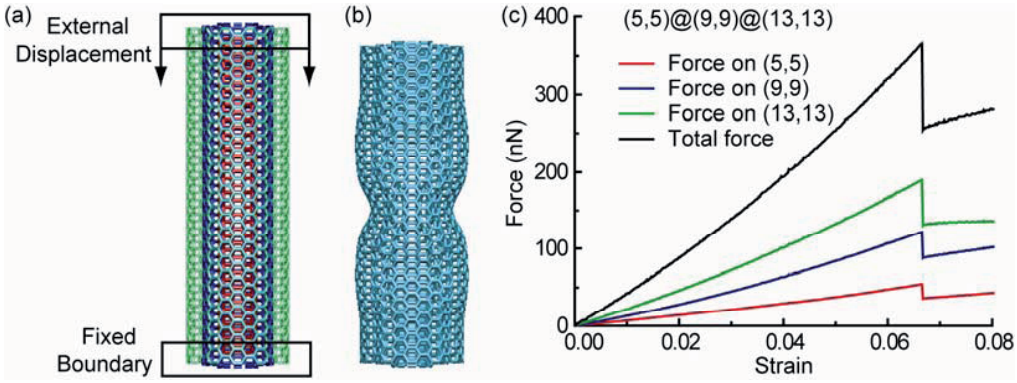

FIG. 1: (a) Front view of geometrical and computational model. **(b)** A typical buckling configuration of PS-TWCNT ((5,5)@(9,9)@(13,13)). **(c)** Corresponding force–strain curve.

Depending on their aspect ratio, SWCNTs could have three buckling modes (Buehler et al., 2004), named shell buckling, Euler buckling and wire-like behavior. To preserve the shell-like failure mode, the effective length of the tube (the length of the unconstrained part in the tube) is chosen to be 4.8 nm for all tubes in our study.

3. CONTINUUM MECHANICS MODEL

Since the van der Waals (vdW) interaction between layers in PS-MWCNTs is more prominent than in normal MWCNTs and could not be neglected (Liew et al., 2007), an continuum mechanics model including the van der Waals interaction among all layers is necessary. Here, we adopt an elastic shell model combined with a refined vdW force model proposed by (He et al., 2005a, 2005b) to study the buckling of PS-MWCNTs.

We study a MWCNT composed of two or more layers with a radius R_i, thickness h, and modulus of elasticity E. The MWCNT is empty inside, and no internal or external lateral pressures are applied to the tube except for the pressure that is caused by the vdW interaction. Based on the classical thin-shell theory (Timoshenko and Gere, 1961), the governing equation for the elastic buckling of a cylindrical shell can be expressed as (He et al., 2005a, 2005b)

$$D\nabla^8 w = \nabla^4 p + N_x \frac{\partial^2}{\partial x^2}\nabla^4 w + \frac{N_\theta}{R^2}\frac{\partial^2}{\partial \theta^2}\nabla^4 w - \frac{Eh}{R^2}\frac{\partial^4 w}{\partial x^4}, \tag{1}$$

where x and θ are the axial and circumferential coordinates, respectively, p the net normal pressure, w the radial deflection, N_x and N_θ the uniform axial and circumferential membrane forces prior to buckling, respectively, D the effective bending stiffness of the tube, and

$$\nabla^2 = \frac{\partial^2}{\partial x^2} + \frac{1}{R^2}\frac{\partial^2}{\partial \theta^2}. \tag{2}$$

Applying Eq. (1) to each of the concentric tubes in the MWCNT, the governing equations for the elastic buckling of the MWNT can be obtained as

$$\begin{aligned} &L_1 w_1 = \nabla_1^4 p_1, \\ &\vdots \\ &L_i w_i = \nabla_i^4 p_i, \\ &\vdots \\ &L_N w_N = \nabla_N^4 p_N, \end{aligned} \tag{3}$$

where w_i (i = 1, 2, ..., N) is the deflection of the ith tube and p_i is the pressure exerted on the ith nanotube due to the vdW interaction between the walls, which can be expressed as

$$p_i(x,\theta) = -\sum_{j=1}^{i-1}\overline{p}_{ij} + \sum_{j=i+1}^{N}\overline{p}_{ij} + \sum_{j=1}^{N}\Delta p_{ij}(x,\theta) \tag{4}$$

where $\overline{p}_{ij}$ is the initial uniform vdW pressure contribution to tube i from tube j prior to buckling, N is the total number of layers of a MWNT, and $\Delta p_{ij}(x,\theta)$ is the pressure increment that is exerted on tube i by tube j, which is assumed to be linearly proportional to the buckling deflection between tube i and tube j (He et al., 2005a, 2005b), i.e.

$$\Delta p_{ij}(x,\theta) = c_{ij}(w_i - w_j), \tag{5}$$

where c_{ij} is the vdW interaction coefficient representing the vdW pressure on tube i from tube j due to the jump of the buckling deflection.

Applying the more refined vdW model suggested by (He et al., 2005a, 2005b), the initial pressure $\overline{p}_{ij}(x,\theta)$ and the vdW interaction coefficient c_{ij} can be obtained in terms of a Lennard-Jones pair potential V_{LJ} as follows:

$$\overline{p}_{ij} = \left[\frac{2048\varepsilon\sigma^{12}}{9a^4}\sum_{k=0}^{5}\frac{(-1)^k}{2k+1}\binom{5}{k}E_{ij}^{12} - \frac{1024\varepsilon\sigma^6}{9a^4}\sum_{k=0}^{2}\frac{(-1)^k}{2k+1}\binom{2}{k}E_{ij}^{6}\right]R_j \tag{6}$$

and

$$c_{ij} = -\left(\frac{1001\pi\varepsilon\sigma^{12}}{3a^4}E_{ij}^{13} - \frac{1120\pi\varepsilon\sigma^{6}}{9a^4}E_{ij}^{7}\right)R_j, \tag{7}$$

where a = 0.1396 nm is the C–C bond length, R_j is the radius of tube j, and E_{ij}^{6}, E_{ij}^{7}, E_{ij}^{12}, and E_{ij}^{13} are the elliptical integrals defined by (He et al., 2005a, 2005b):

$$E_{ij}^{m} = (R_i + R_j)^{-m}\int_0^{\pi/2}\frac{d\theta}{(1 - K_{ij}\cos^2\theta)^{m/2}} \tag{8}$$

and

$$K_{ij} = \frac{4R_iR_j}{(R_i + R_j)^2} \tag{9}$$

The governing equations (3) are coupled with each other only due to the vdW interaction. The more refined vdW model can capture the effects of all of the layers, not just those between two adjacent layers. Since the interlayer distance of PS-MWCNTs is smaller than the normal MWCNTs, this consideration of vdW interaction is critical for the CM model.

For an axially compressed MWCNT composed of an individual tube which is treated as a cylindrical shell with a radius R_i and stiffness Eh, the ends of all of the tubes are assumed to be simply supported, as the buckling analysis is not sensitive to the boundary conditions (Timoshenko and Gere, 1961). The buckling modes of all of the tubes can be approximated as (He et al., 2005a, 2005b)

$$w_k = A_k \sin\frac{m\pi x}{L}\cos n\theta, \tag{10}$$

where A_k (k = 1, 2, ..., N) are unknown coefficients, m and n are the axial half-wave number and the circumferential wave number, respectively, and L is the length of the MWCNT (He et al., 2005a, 2005b).

Substituting Eq. (10) into Eqs. (3) yields a set of equations with N unknowns of A_k (k = 1, 2,..., N) as follows

$$\left[-B_{N\times N} - N_x\left(\frac{m\pi}{L}\right)^2\mathbf{I}_{N\times N}\right]\begin{Bmatrix} A_1 \\ A_2 \\ \vdots \\ A_N \end{Bmatrix} = 0 \tag{11a}$$

where $\boldsymbol{I}_{N\times N}$ is an identity matrix and the elements of the matrix $\boldsymbol{B}_{N\times N}$ are $b_{ij} = c_{ij}$, $i \neq j$, and

$$b_{kk} = D\left[\left(\frac{m\pi}{L}\right)^2 + \left(\frac{n}{R_k}\right)^2\right]^2 - \sum_{\substack{j=1 \\ j\neq k}}^{N} c_{kj} - p_kR_k\left(\frac{n}{R_k}\right)^2 + \frac{Eh}{R_k^2}\left[\frac{1}{1 + (Ln/m\pi R_k)^2}\right]^2 \tag{11b}$$

By solving the following eigenvalue equation,

$$\det\left[-[B] - Nx\left(\frac{m\pi}{L}\right)^2[I]\right] = 0 \tag{12}$$

we can obtain A_k, the buckling amplitude for the kth layer. The buckling membrane force N_x could also be obtained with regard to m and n by choosing the lowest eigenvalues.

4. RESULTS AND DISCUSSION

We first validate our simulation model by comparing the buckling strain of single-walled carbon nanotubes (SWCNTs) derived from our simulation to one of the well-developed continuum models (Yakobson et al., 1996). For short SWCNTs with shell-like local buckling mode, the buckling strain ε_c depends little on the length and can be estimated using

$$\varepsilon_c = \left(2\sqrt{3}\right)\left(1-\upsilon^2\right)^{-1/2} hd^{-1} \tag{13}$$

where υ = 0.19 is the Poisson ratio (Yakobson et al., 1996), h = 0.066–0.089 nm is the thickness of the CNT layer (Kudin et al., 2001; Peng et al., 2008; Wang, et al., 2005; Yakobson et al., 1996) and d is the diameter of SWCNT. From Fig. 2, it is evident that our MM simulation results agree well with the theoretical predictions.

Having validated our simulation model, we start our investigation with PS-DWCNTs. The buckling membrane force, N_{MM}, as a function of inter-layer distance is shown in Fig. 3 and the chiralities of the corresponding DWCNTs are listed in Table 1. For PS-DWCNTs with the same inner tube but different interlayer distance, i.e. (5,5)@(8,8), (5,5)@(9,9) and (5,5)@(10,10), N_{MM} increases as the interlayer distance decreases, which is the same as concluded by Liew et al. (2007) and Zhang et al. (2007). If all the MM results for PS-DWCNTs are considered, then N_{MM} does not change monotonically with respect to interlayer distance. However, if we compare the buckling membrane force

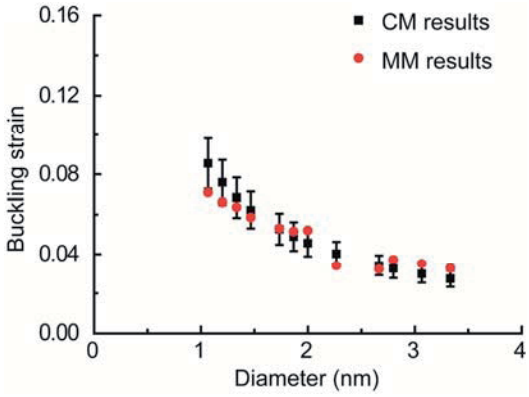

FIG. 2: A comparison between the buckling strain obtained by our MM simulation and that derived from the continuum mechanics (CM) model (Yakobson et al., 1996).

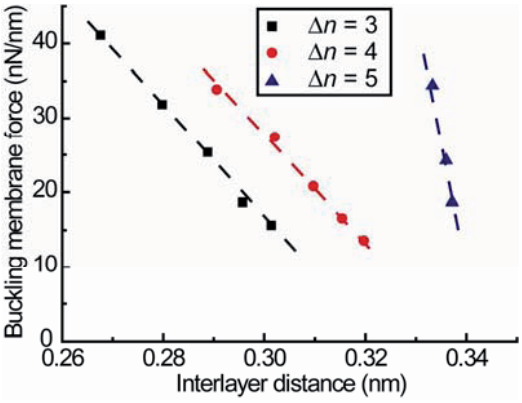

FIG. 3: Buckling membrane force of PS-DWCNTs versus interlayer distance calculated by MM simulation. The dashed lines are used for guiding the eyes.

TABLE 1: The chiralities of DWCNTs (n_1, n_1)@(n_2, n_2) shown in Fig. 1 (for $\Delta n = n_2 - n_1$ = 3, 4, 5, the indices are shown from left to right)

	Squares					**Circles**					**Triangles**		
n_1	5	8	11	14	17	5	9	13	17	21	5	10	15
n_2	8	11	14	17	20	9	13	17	21	25	10	15	20

of PS-DWCNTs with a given intertube chirality difference, we can still find a monotonic relation between N_{MM} and inter-layer distance. Figure 3 demonstrates the dependence of N_{MM} on interlayer distance for PS-DWCNTs with chiralities (n_1, n_1)@(n_2, n_2), where $\Delta n = n_2 - n_1$ = 3, 4, 5, respectively. Such dependence could be explained in terms of the combined effects of diameter and interlayer distance. Using MM simulation, Wang et al. (2005) show that for SWCNTs with same length but different diameters, N_{MM} decreases as diameter increases. Keeping this in mind, for DWCNTs with the same Δn shown in Fig. 3, the decrease of N_{MM} is thus reasonable as the diameters of the tubes increase from left to right (Table 1). However, since N_{MM} also decreases as interlayer increases as found by Zhang et al. (2007) during their investigation on DWCNTs with the same outer tube but different inner tubes, the trend of N_{MM} shown in Fig. 3 should be the results of both the diameter change and interlayer distance variation.

To check whether the two conclusions drawn from PS-DWCNT are still valid for PS-MWCNT, we calculate the buckling membrane force of PS-MWCNTs using MM simulation. The chiralities of PS-TWCNTs and PS-MWCNTs with more than three layers are listed in Tables 2 and 3 respectively. From Fig. 4, it is evident that we can draw the same conclusions as that from PS-DWCNTs. Besides this, it is further found that for PS-MWCNTs with the same innermost tube (connected with black dashed lines in Fig. 4), the buckling membrane force decreases as the number of layers increases, which is consistent with that reported by (Zhang et al., 2008).

Although MM simulation could reveal the mechanisms of PS-MWCNTs on atomic level, it will become very computing intensive if we study PS-MWCNTs over a much wider range to check the universality of the above-mentioned three conclusions derived from our MM simulation based on certain types of PS-MWCNTs. For example, checking whether the results are chirality dependent could be very time consuming as there are numerous combinations of chiralites for CNTs with a given diameter. At this point, continuum mechanics (CM) could play a significant role as it has been shown to possess high efficiency while not losing accuracy (He et al., 2005a, 2005b; Wang et al., 2010).

TABLE 2: The chiralities of three-walled CNTs (TWCNTs) shown in Fig. 2 from left to right

	Three-walled CNTs					
n_1	5	9	13	17	5	10
n_2	9	13	17	21	10	15
n_3	13	17	21	25	15	20

TABLE 3: The chiralities of QWCNTs, 5WCNTs and 6WCNTs shown in Fig. 2 from left to right

	Quad-walled CNTs (QWCNTs)				**5WCNTs**		**6WCNTs**
N_1	5	9	13	5	5	9	5
N_2	9	13	17	10	9	13	9
N_3	13	17	21	15	13	17	13
N_4	17	21	25	20	17	21	17
N_5					21	25	21
N_6							25

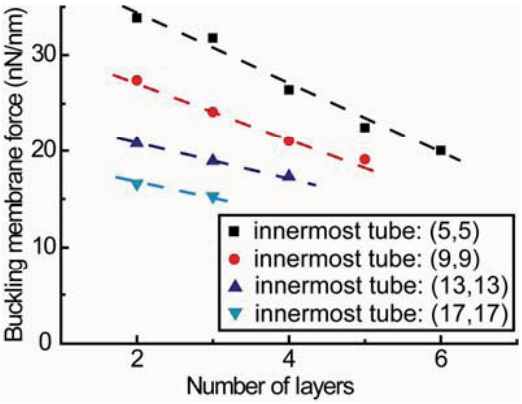

FIG. 4: Buckling membrane force of PS-MWCNTs with different numbers of layers. The difference between the chiralities of each layer is a constant, i.e., $\Delta n = 4$. Different symbols stand for PS-MWCNT with different innermost tubes respectively. The dashed lines are used for guiding the eyes.

Next, we will use CM model to check the validity of the conclusions drawn from our MM simulations and try to gain some insights on the nanoscale level.

By using the aforementioned multi-shell continuum model proposed by (He et al., 2005a, 2005b), we are able to calculate the buckling membrane force of PS-MWCNTs, N_{CM}. The length of PS-MWCNTs, L, is 4.8 nm and the radius of each layer in PS-MWCNTs, R_i, is calculated from energy minimized PS-MWCNTs without any external load using MM simulation as shown in Table 4. In the analysis using the CM model, it is assumed that ε = 0.00284 eV, σ = 0.34 nm for the Lennard-Jones potential and a = 0.1396 nm for the carbon–carbon bond length. It is further assumed that the effective bending stiffness is D = 0.85 eV and Eh = 360 J/m^2 (Liew et al., 2004, 2007).

The buckling membrane force N_{CM} of PS-DWCNTs predicted by the CM model is shown in Fig. 5(a). First, it is evident that the two conclusions drawn from our MM simulation are still valid, which means they are chirality independent. Furthermore, to our surprise, N_{CM} is found to be almost proportional to N_{MM}. To check whether this proportionality still holds for PS-MWCNTs, we plot the N_{MM}/N_{CM} vs. intertube distance curve as shown in Fig. 5(b). It appears that N_{MM}/N_{CM} is almost constant with a value of about 1.5. The consistency between the MM simulation and CM model in sense of the validity of the three conclusions drawn from MM simulation and the universality of the proportionality enables us to study the buckling behavior of PS-MWCNTs in a much wider range.

It would beyond the scope of the current work to quantitatively investigate the difference between the values of N_{MM} and N_{CM}. Here we provide some possible reasons for the difference between MM and CM results. First, the buckling membrane force derived from the CM model corresponds to a "global" minimum energy of the system, while the one calculated by MM is probably a local minimum, as the energy minimization method might not be able to check all of the possible configurations (Cao and Chen, 2006). Second, the CM model assumes that tensile stiffness Eh and bending stiffness D are the same for all the layers. For small diameter SWCNTs, this assumption could be inappropriate (Wang, et al., 2005). We note that a similar phenomenon in which the buckling strain/stress predicted by MM simulations is larger than that predicted by the CM model is also reported in (He et al., 2005b).

5. CONCLUSIONS

In this paper, we first study the buckling behavior of PS-MWCNTs with two to six layers using MM simulation. Taking interlayer distance as the key factor, we show three features of the buckling properties of PS-MWCNTs subjected to axial loading: (1) the buckling membrane force is not a monotonic function of interlayer distance, depending on the nanotube index (i.e. diameter); (2) the buckling membrane force increases as the interlayer distance decreases for PS-MWCNTs with a fixed intertube chirality, which is a combined effect of interlayer distance and tube diameter;

TABLE 4: The initial energy optimized configurations of PS-MWCNTs

	Radius of innermost tube (nm)	Interlayer distance (nm)
(5,5)@(9,9)	0.3296	0.2906
(9,9)@(13,13)	0.5891	0.3021
(13,13)@(17,17)	0.8514	0.3097
(17,17)@(21,21)	1.1151	0.3154
(21,21)@(25,25)	1.3794	0.3197
(5,5)@(10,10)	0.3377	0.3333
(10,10)@(15,15)	0.6688	0.336
(15,15)@(20,20)	1.0016	0.3372
(5,5)@(8,8)	0.3174	0.2676
(8,8)@(11,11)	0.5077	0.2798
(11,11)@(14,14)	0.701	0.2888
(14,14)@(17,17)	0.896	0.2957
(17,17)@(20,20)	1.0921	0.3014
(5,5)@(10,10)@(15,15)	0.3377	0.3319/0.3353
(10,10)@(15,15)@(20,20)	0.6687	0.3342/0.3361
(5,5)@(9,9)@(13,13)	0.3254	0.2820/0.2943
(9,9)@(13,13)@(17,17)	0.5815	0.2930/0.3012
(13,13)@(17,17)@(21,21)	0.8406	0.3005/0.3068
(17,17)@(21,21)@(25,25)	1.1012	0.3065/0.3113
(5,5)@(10,10)@(15,15)@(20,20)	0.3376	0.3319/0.3334/0.3360
(5,5)@(9,9)@(13,13)@(17,17)	0.3227	0.2777/0.2848/0.2981
(9,9)@(13,13)@(17,17)@(21,21)	0.5763	0.2882/0.2917/0.3030
(13,13)@(17,17)@(21,21)@(25,25)	0.8327	0.2959/0.2973/0.3071
(5,5)@(9,9)@(13,13)@(17,17)@(21,21)	0.3209	0.2748/0.2803/0.2881/0.3011
(9,9)@(13,13)@(17,17)@(21,21)@(25,25)	0.5722	0.2854/0.2868/0.2929/0.3050
(5,5)@(9,9)@(13,13)@(17,17)@(21,21)@(25,25)	0.3193	0.2729/0.2771/0.2832/0.2910/0.3038

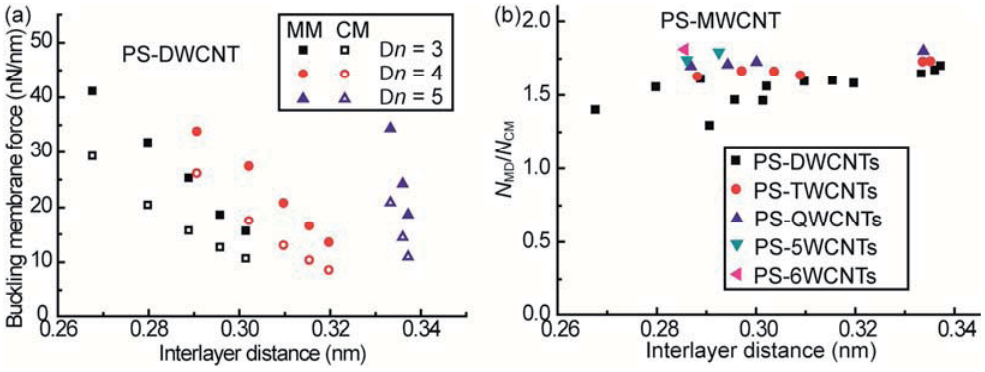

FIG. 5: (a) Comparison of the buckling membrane force of PS-DWCNTs between MM results and continuum model results. **(b)** Ratio of the buckling membrane force predicted by our MM simulation N_{MM} with respect to that calculated using continuum model N_{CM}.

(3) for PS-MWCNTs with the same innermost tube, the buckling membrane force increases as the number of walls increases. To check the universality of the above-mentioned three conclusions, we use a multi-shell continuum model that is combined with a refined vdW force model to study the buckling behavior of PS-MWCNTs. By taking the energy minimized, load-free configurations calculated by MM simulation as input parameters, we find an agreement between the MM simulation results and CM model results, which indicates that the three conclusions are independent of the chiralities of the PS-MWCNTs. Furthermore, we show that the buckling membrane force predicted by CM model is proportional to that of MM simulation. This linear relation is worth being investigated in the future as it relates some fundamental continuum mechanical quantities of PS-MWCNTs to the MM results, and we believe our results could provide theoretical guidance for the design of PS-MWCNTs as compressible materials.

ACKNOWLEDGMENTS

L.S. would like to acknowledge the partial support from the Australian Research Council under Grant No DP0772478. Some simulations were carried out on the supercomputers in the Victorian Partnership for Advanced Computing (VPAC) and the NCI National Facility in Australia.

REFERENCES

Brenner, D. W., Shenderova, O. A., Harrison, J. A., Stuart, S. J., Ni, B., and Sinnott, S. B., A second-generation reactive empirical bond order (REBO) potential energy expression for hydrocarbons, *J. Phys.-Cond. Matter*, vol. **14**, no. 4, pp. 783–802, 2002.

Buehler, M. J., Kong, Y., and Gao, H. J., Deformation mechanisms of very long single-wall carbon nanotubes subject to compressive loading, *J. Eng. Mater. Technol.—Trans. ASME*, vol. **126**, no. 3, pp. 245–249, 2004.

Cao, G. X. and Chen, X., Buckling behavior of single-walled carbon nanotubes and a targeted molecular mechanics approach, *Phys. Rev. B*, vol. **74**, no. 16, p. 165422, 2006.

Cumings, J. and Zettl, A., Low-friction nanoscale linear bearing realized from multiwall carbon nanotubes, *Science*, vol. **289**, no. 5479, pp. 602–604, 2000.

da Silva, A. J. R., Fazzio, A., and Antonelli, A., Bundling up carbon nanotubes through Wigner defects, *Nano Lett.*, vol. **5**, no. 6, pp. 1045–1049, 2005.

He, X. Q., Kitipornchai, S., and Liew, K. M., Buckling analysis of multi-walled carbon nanotubes: A continuum model accounting for van der Waals interaction, *J. Mech. Phys. Solids*, vol. **53**, no. 2, pp. 303–326, 2005a.

He, X. Q., Kitipornchai, S., Wang, C. M., and Liew, K. M., Modeling of van der Waals force for infinitesimal deformation of multi-walled carbon nanotubes treated as cylindrical shells, *Int. J. Solids Struct.*, vol. **42**, no. 23, pp. 6032–6047, 2005b.

Huhtala, M., Krasheninnikov, A. V., Aittoniemi, J., Stuart, S. J., Nordlund, K., and Kaski, K., Improved mechanical load transfer between shells of multiwalled carbon nanotubes, *Phys. Rev. B*, vol. **70**, no. 4, p. 045404, 2004.

Kis, A., Csanyi, G., Salvetat, J. P., Lee, T. N., Couteau, E., Kulik, A. J., Benoit, W., Brugger, J., and Forro, L., Reinforcement of single-walled carbon nanotube bundles by intertube bridging, *Nature Mater.*, vol. **3**, no. 3, pp. 153–157, 2004.

Kudin, K. N., Scuseria, G. E., and Yakobson, B. I., C2F, BN, and C nanoshell elasticity from ab initio computations, *Phys. Rev. B*, vol. **64**, no. 23, p. 235406, 2001.

Liew, K. M., Wong, C. H., He, X. Q., Tan, M. J., and Meguid, S. A., Nanomechanics of single and multiwalled carbon nanotubes, *Phys. Rev. B*, vol. **69**, no. 11, p. 115429, 2004.

Liew, K. M., Wang, J. B., He, X. Q., and Zhang, H. W., Buckling analysis of abnormal multiwalled carbon nanotubes, *J. Appl. Phys.*, vol. **102**, no. 5, p. 053511, 2007.

Ma, M. D., Liu, J. Z., Wang, L., Shen, L., Xie, L., Wei, F., Zhu, J., Gong, Q., Liang, J., and Zheng, Q., Reversible high-pressure carbon nanotube vessel, *Phys. Rev. B*, vol. **81**, no. 23, p. 235420, 2010.

Mielke, S. L., Troya, D., Zhang, S., Li, J. L., Xiao, S. P., Car, R., Ruoff, R. S., Schatz, G. C., and Belytschko, T., The role of vacancy defects and holes in the fracture of carbon nanotubes, *Chem. Phys. Lett.*, vol. **390**, nos. 4–6, pp. 413–420, 2004.

Mielke, S. L., Belytschko, T., and Schatz, G. C., Nanoscale fracture mechanics, *Ann. Rev. Phys. Chem.*, vol. **58**, pp. 185–209, 2007.

Oberlin, A., Endo, M., and Koyama, T., Filamentous growth of carbon through benzene decomposition, *J. Crystal Growth*, vol. **32**, no. 3, pp. 335–349, 1976.

Peng, J., Wu, J., Hwang, K. C., Song, J., and Huang, Y., Can a single-wall carbon nanotube be modeled as a thin shell? *J. Mech. Phys. Solids*, vol. **56**, no. 6, pp. 2213–2224, 2008.

Plimpton, S., Fast parallel algorithms for short-range molecular-dynamics, *J. Comput. Phys.*, vol. **117**, no. 1, pp. 1–19, 1995.

Sammalkorpi, M., Krasheninnikov, A., Kuronen, A., Nordlund, K., and Kaski, K., Mechanical properties of carbon nanotubes with vacancies and related defects, *Phys. Rev. B*, vol. **70**, no. 24, p. 245416, 2004.

Stuart, S. J., Tutein, A. B., and Harrison, J. A., A reactive potential for hydrocarbons with intermolecular interactions, *J. Chem. Phys.*, vol. **112**, no. 14, pp. 6472–6486, 2000.

Sun, L., Banhart, F., Krasheninnikov, A. V., Rodriguez-Manzo, J. A., Terrones, M., and Ajayan, P. M., Carbon nanotubes as high-pressure cylinders and nanoextruders, *Science*, vol. **312**, no. 5777, pp. 1199–1202, 2006.

Timoshenko, S. P. and Gere, J. M., *Theory of Elastic Stability*, New York: McGraw-Hill, 1961.

Wang, C. M., Zhang, Y. Y., Xiang, Y., and Reddy, J. N., Recent studies on buckling of carbon nanotubes, *Appl. Mech. Revs.*, vol. **63**, no. 3, p. 030804, 2010.

Wang, L. F., Zheng, Q. S., Liu, J. Z., and Jiang, Q., Size dependence of the thin-shell model for carbon nanotubes, *Phys. Rev. Lett.*, vol. **95**, no. 10, p. 105501, 2005.

Wang, L. F., Ph.D. Thesis, Tsinghua University, Beijing, 2006.

Wang, Y., Wang, X. X., Ni, X. G., and Wu, H. A., Simulation of the elastic response and the buckling modes of single-walled carbon nanotubes, *Comput. Mater. Sci.*, vol. **32**, no. 2, pp. 141–146, 2005.

Xia, Z. H., Guduru, P. R., and Curtin, W. A., Enhancing mechanical properties of multiwall carbon nanotubes via *sp*(3) interwall bridging, *Phys. Rev. Lett.*, vol. **98**, no. 24, p. 245501, 2007.

Xu, Z. P., Wang, L. F., and Zheng, Q. S., Enhanced mechanical properties of prestressed multi-walled carbon nanotubes, *Small*, vol. **4**, no. 6, pp. 733–737, 2008.

Yakobson, B. I., Brabec, C. J., and Bernholc, J., Nanomechanics of carbon tubes: Instabilities beyond linear response, *Phys. Rev. Lett.*, vol. **76**, no. 14, pp. 2511–2514, 1996.

Yu, M. F., Lourie, O., Dyer, M. J., Moloni, K., Kelly, T. F., and Ruoff, R. S., Strength and breaking mechanism of multiwalled carbon nanotubes under tensile load, *Science*, vol. **287**, no. 5453, pp. 637–640, 2000a.

Yu, M. F., Yakobson, B. I., and Ruoff, R. S., Controlled sliding and pullout of nested shells in individual multiwalled carbon nanotubes, *J. Phys. Chem. B*, vol. **104**, no. 37, pp. 8764–8767, 2000b.

Zhang, H. W., Wang, L., and Wang, J. B., Computer simulation of buckling behavior of double-walled carbon nanotubes with abnormal interlayer distances, *Comput. Mater. Sci.*, vol. **39**, no. 3, pp. 664–672, 2007.

Zhang, Y. Y., Wang, C. M., and Tan, V. B. C., Examining the effects of wall numbers on buckling behavior and mechanical properties of multiwalled carbon nanotubes via molecular dynamics simulations, *J. Appl. Phys.*, vol. **103**, no. 5, p. 053505, 2008.